Available online at www.sciencedirect.com
ScienceDirect
Journal of Sound and Vibration 298 (2006) 333–349
JOURNAL OF SOUND AND VIBRATION
www.elsevier.com/locate/jsvi

Free vibration of laminated composite and sandwich plates using global–local higher-order theory ☆

Wu Zhen, Chen Wanji*

State Key Laboratory for Structural Analysis of Industrial Equipment, Dalian University of Technology, Dalian 116023, PR China

Received 19 October 2005; received in revised form 10 March 2006; accepted 22 May 2006
Available online 4 August 2006

Abstract

In this paper the global–local higher-order theory is used to study the free vibration of laminated composite and sandwich plates. This global–local theory can satisfy the free surface conditions and the geometric and stress continuity conditions at interfaces, and the number of unknowns is independent of the layer numbers of the laminate. Based on the higher-order theory, a refined three-noded triangular element satisfying C^1 weak-continuity conditions is presented. For general laminated composite plates, results obtained from present global–local higher-order theory have been found in good agreement with those obtained from three-dimensional elasticity theories. Moreover, this theory is still suitable for analysis of laminated plates with arbitrary layouts and soft-core sandwich plates whereas numerical results show that the global higher-order and first-order theory overestimate natural frequency for these special structures. This theory cannot only calculate the natural frequencies but can accurately predict the modal stress distributions in the thickness direction without any smooth techniques.

1. Introduction

Laminated composite and sandwich plates are being increasingly used in advanced aerospace structures because they can exhibit many favorable characteristics such as high specific modulus and strength and low specific density. To use them efficiently, it is necessary to develop appropriate models capable of accurately predicting their structural and dynamical behavior.

Due to ignoring the transverse shear deformation and overestimating the natural frequency, the classical laminate plate theory becomes inadequate for the analysis of thick laminated and sandwich plates. Therefore it is necessary to consider the effect of transverse shear deformation in the study of thick laminated structures. To take into account the effects of shear deformation, the first-order shear deformation theories [1,2] are firstly developed whereas the accuracy of solutions of this theory will be strongly dependent on the shear correction factors. In order to overcome the limitations of first-order shear deformation theory, the global higher-order theories that include higher-order terms in Taylor's expansions of the displacement in

☆Contract/grant sponsor: National Natural Sciences Foundation of China (No. 50479058).
*Corresponding author.
E-mail address: chenwj@dlut.edu.cn (C. Wanji).

0022-460X/$ - see front matter © 2006 Elsevier Ltd. All rights reserved.
doi:10.1016/j.jsv.2006.05.022

the thickness direction have been developed by Reddy [3], Frederiksen [4], Maiti and Sinha [5], Kant and Swaminathan [6,7], Lee et al. [8] and Matsunaga [9–11]. In addition, based on Reddy's higher-order theories, finite element method [12] has been also proposed. Compared with first-order theories, the higher-order theories are more accurate in predicting natural frequencies for general laminated plates [6,7]. Therefore, prevalent view is that the global higher-order theories are enough for analyzing dynamical problems of laminated structures.

However, by further research, it is found that the global higher-order theories also overestimate natural frequency for laminated composite plates with different thickness and materials at each ply [13] and soft-core sandwich plates [14] because these higher-order theories violate continuity conditions of the transverse stress components. To overcome the drawbacks of global higher-order theories, the layerwise theories [15–18] have been used to perform free vibration analysis of laminated plates. Subsequently mixed layerwise models [19,20] have been also proposed, which assumed that the transverse stresses and displacement unknowns in each layer are two independent fields. It should be shown that the layerwise models are accurate enough in predicting natural frequencies of arbitrary laminated structures whereas these models are computationally expensive because the number of unknown functions depends on the number of layers of the laminate. On the other hand, Kapuria et al. [13] present a zig-zag theory of laminated beams to assess the effect of laminate layouts on the accuracy whereas the research on laminated and sandwich plates is not given using this zig-zag theory. To the best of the author's knowledge, other investigations on the free vibration of sandwich plates cannot be found using zig-zag theories.

To overcome the limitations of the global higher-order theories and layerwise theories, this paper is to use the global–local theory to predict dynamical response of laminated composite plates with arbitrary layout and soft-core sandwich plates. The global–local higher-order theory is firstly developed by Li and Liu [21] and further study on the global–local theory has been presented by Wu et al. [22,23]. This theory possesses the accuracy of layerwise theory and efficiency of global higher-order theory, moreover, which satisfies displacements and transverse shear stresses continuity conditions at the interfaces. It is most important that the in-plane stresses and transverse shear stresses can be accurately predicted by the direct constitutive equation approach without any smooth techniques. Based on the global–local higher-order theory, the refined triangular plate element is presented. Due to second derivatives of transverse displacement appearing in higher-order shear deformation theory, the interelement C^1 continuity conditions should been imposed. In order to satisfy this C^1 continuity conditions, the refined triangular nonconforming methods [24,25] have been employed in this paper.

2. Global–local higher-order theory review

In this section, a global–local higher-order theory for laminated composite and sandwich plates is briefly reviewed. The detailed description can be found in the previous works [21–23]. The starting displacement field can be written as follows:

$$u^k(x,y,z) = u_G(x,y,z) + \bar{u}_L^k(x,y,z) + \hat{u}_L^k(x,y,z), \tag{1a}$$

$$v^k(x,y,z) = v_G(x,y,z) + \bar{v}_L^k(x,y,z) + \hat{v}_L^k(x,y,z), \tag{1b}$$

$$w^k(x,y,z) = w_G(x,y,z), \tag{1c}$$

where u_G, v_G and w_G are global components of displacement expansion; $\bar{u}_L^k$ and $\bar{v}_L^k$ are of two-term local groups; $\hat{u}_L^k$ and $\hat{v}_L^k$ are of one-term local group; the superscript k represents the layer order of laminated plates. The global coordinates associated with the plate are x, y, z. The reference plane ($z = 0$) is taken at the mid-plane of the laminate. The local coordinates for a layer are denoted by x, y, ζ_k where $-1 \leqslant \zeta_k \leqslant 1$. The relations between global coordinate and local coordinate can be seen in Fig. 1.

These global components may be written as

$$u_G(x,y,z) = u_0(x,y) + zu_1(x,y) + z^2u_2(x,y) + z^3u_3(x,y), \tag{2a}$$

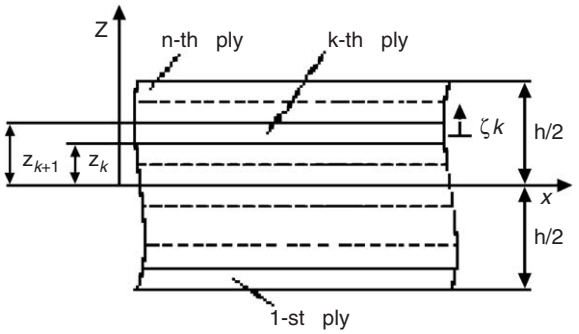

Fig. 1. Schematic figure for the laminate segment.

$$v_G(x,y,z) = v_0(x,y) + zv_1(x,y) + z^2v_2(x,y) + z^3v_3(x,y), \tag{2b}$$

$$w_G(x,y,z) = w_0(x,y). \tag{2c}$$

The local components can be written as

$$\bar{u}_L^k(x,y,z) = \zeta_k u_1^k(x,y) + \zeta_k^2 u_2^k(x,y), \tag{3a}$$

$$\bar{v}_L^k(x,y,z) = \zeta_k v_1^k(x,y) + \zeta_k^2 v_2^k(x,y), \tag{3b}$$

$$\hat{u}_L^k(x,y,z) = \zeta_k^3 u_3^k(x,y), \tag{3c}$$

$$\hat{v}_L^k(x,y,z) = \zeta_k^3 v_3^k(x,y), \tag{3d}$$

where

$$\zeta_k = a_k z - b_k; \quad a_k = \frac{2}{z_{k+1} - z_k}; \quad b_k = \frac{z_{k+1} + z_k}{z_{k+1} - z_k}.$$

By enforcing free conditions of the transverse shear stresses on the top and bottom surfaces, and displacements and transverse shear stresses continuity conditions at the interfaces, the final displacement field reduces to the following form:

$$u^k = u_0 + \Phi_1^k(z)u_1^1 + \Phi_2^k(z)u_1 + \Phi_3^k(z)u_2 + \Phi_4^k(z)u_3 + \Phi_5^k w_{0,x}, \tag{4a}$$

$$v^k = v_0 + \Psi_1^k(z)u_1^1 + \Psi_2^k(z)u_1 + \Psi_3^k(z)u_2 + \Psi_4^k(z)u_3 + \Psi_5^k w_{0,x}, \tag{4b}$$

$$w^k = w_0, \tag{4c}$$

where Φ_i^k and ψ_i^k are the function of material constants and thickness of laminated plate. The expression of Φ_i^k and ψ_i^k is found in Refs. [22,23].

3. The transverse displacement function of element

The global–local higher-order theory possesses first and second derivatives of transverse displacement w in the strain components. Thus the C^0 and C^1 continuity displacement functions should be used. To satisfy these continuity conditions, the famous nine-parameter nonconforming element BCIZ [26] satisfied C^0 continuity condition and the refined nonconforming element method developed by Chen Wanji et al. [24,25] are used in the present study, respectively.

Based on the refined element method [24], the displacement function w^* satisfied C^1 weak-continuity condition may be expressed as

$$w^* = w^0 + P\alpha \tag{5}$$

where w^0 is a nonconforming displacement function; $P = \left|\frac{1}{2}x^2 \quad \frac{1}{2}y^2 \quad xy\right|$; α is unknown parameter.

Following partial integration is used:

$$\int_{v_e} \frac{\partial^2 w^*}{\partial x_i \partial x_j} \mathrm{d}x\,\mathrm{d}y = \oint_{\partial v_e} \frac{\partial \tilde{w}}{\partial x_i} n_{xj}\,\mathrm{d}s \quad (i,j=1,2), \tag{6}$$

where $\tilde{w}$ is the interpolation of displacement on the element boundary, which relaxes conforming condition; n_{xj} is the cosines of the vector normal to the coordinate x_j.

Substituting Eq. (5) into Eq. (6), the following expression can be obtained:

$$\int_{v_e} D^{\mathrm{T}} w^*\,\mathrm{d}x\,\mathrm{d}y = \int_{v_e} \left(D^{\mathrm{T}} w^0 + \alpha\right) \mathrm{d}x\,\mathrm{d}y = \Delta(B_0 q + \alpha) = \oint_{v_e} R_c^{\mathrm{T}} \tilde{u}\,\mathrm{d}s \tag{7}$$

where,

$$D^{\mathrm{T}} = \left\{ \frac{\partial^2}{\partial x^2} \quad \frac{\partial^2}{\partial y^2} \quad \frac{\partial^2}{\partial x \partial y} \right\}^{\mathrm{T}},\ D^{\mathrm{T}} w^0 = Bq,\ B_0 = \frac{1}{\Delta} \int_{v^e} B\,\mathrm{d}x\,\mathrm{d}y;$$

Δ is element area;

$$R_c^{\mathrm{T}} = \begin{bmatrix} \ell^2 & -\ell m \\ m^2 & \ell m \\ \ell m & (\ell^2 - m^2)/2 \end{bmatrix};\quad \tilde{u} = \begin{Bmatrix} \dfrac{\partial \tilde{w}}{\partial n} \\ \dfrac{\partial \tilde{w}}{\partial s} \end{Bmatrix},$$

where ℓ and m are the cosines of the vector normal on the boundaries.

By simplifying, the following equation can be written as

$$\oint_{v_e} R_c^{\mathrm{T}} \tilde{u}\ \mathrm{d}s = \Delta B_c q. \tag{8}$$

By using Eqs. (7) and (8), the unknown parameter α may be obtained directly as

$$\alpha = (B_c - B_0) q. \tag{9}$$

Therefore the displacement function w^* satisfied C^1 weak-continuity conditions can be given as

$$w^* = w^0 + P(B_c - B_0) q. \tag{10}$$

4. The refined three-node triangular laminated plate element

4.1. The element transverse displacement function satisfied C^0 continuity condition

The famous nine-parameter nonconforming element BCIZ [26] satisfies C^0 continuity condition, which may be written as follows:

$$w^0 = Fq, \tag{11}$$

where

$$F = \left\lfloor F_i, F_{xi}, F_{yi} \right\rfloor,\ q = \{w_i^0, w_{xi}^0, w_{yi}^0\}^{\mathrm{T}},$$

$$F_i = L_i + L_i^2 L_j + L_i^2 L_k - L_i L_j^2 - L_i L_k^2;\ F_{xi} = c_k L_i^2 L_j - c_j L_i^2 L_k + (c_k - c_j) L_i L_j L_k / 2,$$

$$F_{yi} = b_j L_i^2 L_k - b_k L_i^2 L_j + (b_j - b_k) L_i L_j L_k / 2;\ L_i = \frac{a_i + b_i x + c_i y}{2\Delta},\ a_i = x_j y_k - x_k y_j,$$

$$b_i = y_j - y_k,\ c_i = x_k - x_j (i = 1 - 3).$$

Second order derivatives of transverse displacement w^0 may be given as

$$\left\{ \frac{\partial^2 w^0}{\partial x^2} \quad \frac{\partial^2 w^0}{\partial y^2} \quad \frac{\partial^2 w^0}{\partial x \partial y} \right\}^{\mathrm{T}} = Bq, \tag{12}$$

where, $B = [B_1\ B_2\ B_3]$ and

$$B_i = \begin{bmatrix} \dfrac{\partial^2 F_i}{\partial x^2} & \dfrac{\partial^2 F_{xi}}{\partial x^2} & \dfrac{\partial^2 F_{yi}}{\partial x^2} \\ \dfrac{\partial^2 F_i}{\partial y^2} & \dfrac{\partial^2 F_{xi}}{\partial y^2} & \dfrac{\partial^2 F_{yi}}{\partial y^2} \\ \dfrac{\partial^2 F_i}{\partial x \partial y} & \dfrac{\partial^2 F_{xi}}{\partial x \partial y} & \dfrac{\partial^2 F_{yi}}{\partial x \partial y} \end{bmatrix} \quad (i = 1 - 3).$$

4.2. The element transverse displacement function satisfied C^1 weak-continuity condition

In order to obtain the shape function of element transverse displacement satisfied C^1 weak-continuity condition, the matrix B_c have to be given according to Eq. (10). Here the matrix B_c can be given as

$$B_c = [B_{c_1} \quad B_{c_2} \quad B_{c_3}]. \tag{13}$$

Along boundary 1–2 and boundary 3–1, $(\partial \tilde{w}/\partial n)$ is obtained by linear interpolation, $(\partial \tilde{w}/\partial s)$ is obtained by quadratic interpolation. After integration, we have

$$B_{c_1} = \begin{bmatrix} \ell_1 m_1 - \ell_3 m_3 & \frac{1}{2}(\ell_1^2 y_{21} + \ell_3^2 y_{13}) & \frac{1}{2}(\ell_1^2 x_{12} + \ell_3^2 x_{31}) \\ \ell_3 m_3 - \ell_1 m_1 & \frac{1}{2}(m_1^2 y_{21} + m_3^2 y_{13}) & \frac{1}{2}(m_1^2 x_{12} + m_3^2 x_{31}) \\ m_1^2 - m_3^2 & \frac{1}{2}(\ell_1^2 x_{12} + \ell_3^2 x_{31}) & \frac{1}{2}(m_1^2 y_{21} + m_3^2 y_{13}) \end{bmatrix}, \tag{14}$$

where, ℓ_i, m_i are the cosines of the vector normal to the ith boundary. $x_{ij} = x_i - x_j$, $y_{ij} = y_i - y_j$, where x_i and y_i are the coordinates of node i.

B_{c_2} and B_{c_3} can be obtained by the permutation of the subscript. According to Eq. (10), the shape function F^* can be obtained as

$$F^* = F + P(B_c - B_0). \tag{15}$$

4.3. The displacement functions of triangular element

The primary displacement unknowns are expressed in terms of nodal variables and shape functions as follows:

$$\begin{aligned} u_0 &= \sum_{i=1}^{3} L_i u_{0i},\ u_1^1 = \sum_{i=1}^{3} L_i u_{1i}^1,\ u_j = \sum_{i=1}^{3} L_i u_{ji}, \\ v_0 &= \sum_{i=1}^{3} L_i v_{0i},\ v_1^1 = \sum_{i=1}^{3} L_i v_{1i}^1,\ v_j = \sum_{i=1}^{3} L_i v_{ji}, \\ w^0 &= \sum_{i=1}^{3} (F_i w_{0,i} + F_{xi} w_{0,xi} + F_{yi} w_{0,yi}), \\ w^* &= \sum_{i=1}^{3} (F_i^* w_{0,i} + F_{xi}^* w_{0,xi} + F_{yi}^* w_{0,yi}), \end{aligned} \tag{16}$$

where, $j = 1-3$ and L_i is area coordinate.

4.4. The strain, stiffness and mass matrix of three-node triangular element

According to linear strain–displacement relations, the strain for the kth layer can be written as follows:

$$\varepsilon^k = \partial u^k = [B_1 \quad B_2 \quad B_3]\delta^e, \tag{17}$$

where, $\delta^e = [\delta_1^e \quad \delta_2^e \quad \delta_3^e]^{\mathrm{T}}$

$$\delta_i^e = [\,u_{0i} \quad v_{0i} \quad w_{0i} \quad u_{1i}^1 \quad u_{1i} \quad u_{2i} \quad u_{3i} \quad w_{0xi} \quad v_{1i}^1 \quad v_{1i} \quad v_{2i} \quad v_{3i} \quad w_{0yi}\,]^{\mathrm{T}} \ (i = 1-3).$$

$$[\partial] = \begin{bmatrix} \dfrac{\partial}{\partial x} & 0 & \dfrac{\partial}{\partial y} & \dfrac{\partial}{\partial z} & 0 \\ 0 & \dfrac{\partial}{\partial y} & \dfrac{\partial}{\partial x} & 0 & \dfrac{\partial}{\partial z} \\ 0 & 0 & 0 & \dfrac{\partial}{\partial x} & \dfrac{\partial}{\partial y} \end{bmatrix}^{\mathrm{T}}.$$

The formation of strain matrix B of the refined nonconforming element has been established. By using the following equation, the element stiffness matrix K^e may be given as

$$[K^e] = \sum_{i=1}^{n} \int_{i-1}^{i} \left(\iint B^{\mathrm{T}} Q_i B \, \mathrm{d}x \ \mathrm{d}y \right) \mathrm{d}z. \tag{18}$$

Using Hamilton's principle, the equation of motion for an element can be obtained as follows:

$$[M^e]\ddot{\delta}^e + [K^e]\delta^e = 0, \tag{19}$$

where $[M^e]$ is the element mass matrix and can be written as

$$[M^e] = \int_{A_e} \int_{-h/2}^{h/2} [N]^{\mathrm{T}}[P][N] \ \mathrm{d}z \ \mathrm{d}A \tag{20}$$

in which the matrix $[N]$ and $[P]$ can be presented, respectively:

$$[N] = [N_1 \quad N_2 \quad N_3], \tag{21}$$

where

$$N_i = \begin{bmatrix} L_i & 0 & 0 & 0 & 0 & 0 & 0 & 0 & 0 & 0 & 0 & 0 & 0 \\ 0 & L_i & 0 & 0 & 0 & 0 & 0 & 0 & 0 & 0 & 0 & 0 & 0 \\ 0 & 0 & F_i & 0 & 0 & 0 & 0 & F_{xi} & 0 & 0 & 0 & 0 & F_{yi} \\ 0 & 0 & 0 & L_i & 0 & 0 & 0 & 0 & 0 & 0 & 0 & 0 & 0 \\ 0 & 0 & 0 & 0 & L_i & 0 & 0 & 0 & 0 & 0 & 0 & 0 & 0 \\ 0 & 0 & 0 & 0 & 0 & L_i & 0 & 0 & 0 & 0 & 0 & 0 & 0 \\ 0 & 0 & 0 & 0 & 0 & 0 & L_i & 0 & 0 & 0 & 0 & 0 & 0 \\ 0 & 0 & F_{i,x} & 0 & 0 & 0 & 0 & F_{xi,x} & 0 & 0 & 0 & 0 & F_{yi,x} \\ 0 & 0 & 0 & 0 & 0 & 0 & 0 & 0 & L_i & 0 & 0 & 0 & 0 \\ 0 & 0 & 0 & 0 & 0 & 0 & 0 & 0 & 0 & L_i & 0 & 0 & 0 \\ 0 & 0 & 0 & 0 & 0 & 0 & 0 & 0 & 0 & 0 & L_i & 0 & 0 \\ 0 & 0 & 0 & 0 & 0 & 0 & 0 & 0 & 0 & 0 & 0 & L_i & 0 \\ 0 & 0 & F_{i,y} & 0 & 0 & 0 & 0 & F_{xi,y} & 0 & 0 & 0 & 0 & F_{yi,y} \end{bmatrix} (i = 1-3),$$

$$[P]=\rho(z)\begin{bmatrix}
1 & 0 & 0 & \Phi_1^k & \Phi_2^k & \Phi_3^k & \Phi_4^k & \Phi_5^k & 0 & 0 & 0 & 0 & 0\\
0 & 1 & 0 & 0 & 0 & 0 & 0 & 0 & \Psi_1^k & \Psi_2^k & \Psi_3^k & \Psi_4^k & \Psi_5^k\\
0 & 0 & 1 & 0 & 0 & 0 & 0 & 0 & 0 & 0 & 0 & 0 & 0\\
\Phi_1^k & 0 & 0 & \Phi_1^k\Phi_1^k & \Phi_1^k\Phi_2^k & \Phi_1^k\Phi_3^k & \Phi_1^k\Phi_4^k & \Phi_1^k\Phi_5^k & 0 & 0 & 0 & 0 & 0\\
\Phi_2^k & 0 & 0 & \Phi_2^k\Phi_1^k & \Phi_2^k\Phi_2^k & \Phi_2^k\Phi_3^k & \Phi_2^k\Phi_4^k & \Phi_2^k\Phi_5^k & 0 & 0 & 0 & 0 & 0\\
\Phi_3^k & 0 & 0 & \Phi_3^k\Phi_1^k & \Phi_3^k\Phi_2^k & \Phi_3^k\Phi_3^k & \Phi_3^k\Phi_4^k & \Phi_3^k\Phi_5^k & 0 & 0 & 0 & 0 & 0\\
\Phi_4^k & 0 & 0 & \Phi_4^k\Phi_1^k & \Phi_4^k\Phi_2^k & \Phi_4^k\Phi_3^k & \Phi_4^k\Phi_4^k & \Phi_4^k\Phi_5^k & 0 & 0 & 0 & 0 & 0\\
\Phi_5^k & 0 & 0 & \Phi_5^k\Phi_1^k & \Phi_5^k\Phi_2^k & \Phi_5^k\Phi_3^k & \Phi_5^k\Phi_4^k & \Phi_5^k\Phi_5^k & 0 & 0 & 0 & 0 & 0\\
0 & \Psi_1^k & 0 & 0 & 0 & 0 & 0 & 0 & \Psi_1^k\Psi_1^k & \Psi_1^k\Psi_2^k & \Psi_1^k\Psi_3^k & \Psi_1^k\Psi_4^k & \Psi_1^k\Psi_5^k\\
0 & \Psi_2^k & 0 & 0 & 0 & 0 & 0 & 0 & \Psi_2^k\Psi_1^k & \Psi_2^k\Psi_2^k & \Psi_2^k\Psi_3^k & \Psi_2^k\Psi_4^k & \Psi_2^k\Psi_5^k\\
0 & \Psi_3^k & 0 & 0 & 0 & 0 & 0 & 0 & \Psi_3^k\Psi_1^k & \Psi_3^k\Psi_2^k & \Psi_3^k\Psi_3^k & \Psi_3^k\Psi_4^k & \Psi_3^k\Psi_5^k\\
0 & \Psi_4^k & 0 & 0 & 0 & 0 & 0 & 0 & \Psi_4^k\Psi_1^k & \Psi_4^k\Psi_2^k & \Psi_4^k\Psi_3^k & \Psi_4^k\Psi_4^k & \Psi_4^k\Psi_5^k\\
0 & \Psi_5^k & 0 & 0 & 0 & 0 & 0 & 0 & \Psi_5^k\Psi_1^k & \Psi_5^k\Psi_2^k & \Psi_5^k\Psi_3^k & \Psi_5^k\Psi_4^k & \Psi_5^k\Psi_5^k
\end{bmatrix}, \tag{22}$$

where $\rho(z)$ is the mass density.

By assembling all the element mass and stiffness matrix with the global coordinates the dynamic equation becomes

$$[M]\ddot{\delta}+[K]\delta=0, \tag{23}$$

where $[M]$ and $[K]$ are the global mass and stiffness matrix, respectively.

Eq. (23) may be expressed as the following eigenvalue problem:

$$([K]-\Omega^2[M])\delta=0 \tag{24}$$

in which δ is the displacement vector.

In the present study, the subspace iteration method [27] is adopted to solve the eigenvalue problem.

5. Numerical examples

In this section, several typical problems of laminated composite and sandwich plates have been analyzed. The main aim is to show the importance of satisfying continuity conditions of displacement as well as the transverse stresses for accurate vibration analysis of laminated and sandwich plates. The mesh configuration can be seen in Fig. 2. The following boundary conditions have been used.

Simply supported boundary:

$$u_0=w_0=u_1^1=u_1=u_2=u_3=\frac{\partial w_0}{\partial x}=0 \text{ at } y=0,L,$$

$$v_0=w_0=v_1^1=v_1=v_2=v_3=\frac{\partial w_0}{\partial y}=0 \text{ at } x=0,L.$$

Clamped boundary:

$$u_0=v_0=w_0=u_1^1=u_1=u_2=u_3=\frac{\partial w_0}{\partial x}=v_1^1=v_1=v_2=v_3=\frac{\partial w_0}{\partial y}=0 \text{ at } x=0,L \text{ and } y=0,L.$$

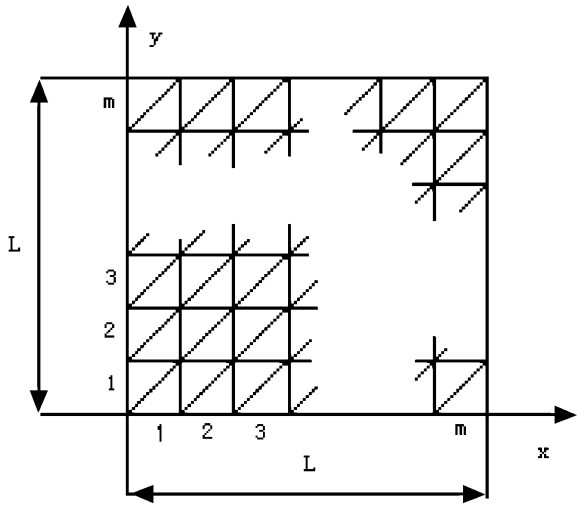

Fig. 2. A full square plate with meshes of $m \times m$.

5.1. Natural frequency of cross-ply (0°/90°/90°/0°) laminated composite plate with simply-free conditions at two opposite edges is analyzed

The plate is simply supported along the edges parallel to the y-axis while the other two edges are free. The following orthotropic material properties have been used

$$E_1 = 181\ \text{GPa}, \quad E_2 = 10.3\ \text{GPa}, \quad E_3 = E_2, \quad G_{12} = G_{13} = 7.17\ \text{GPa},$$
$$G_{23} = 2.87\ \text{GPa} \quad v_{12} = v_{13} = 0.25, \quad v_{23} = 0.33, \quad S = L/h.$$

The material properties are assumed to be the same for all layers. The thickness of each layer is identified and the mass density $\rho = 1578\,\text{kg/m}^3$ is also taken to be uniform in the thickness direction. The natural frequencies are normalized as $\Omega = \omega LS\sqrt{\rho/E_2}$.

In order to verify the present solutions, the convergence properties of the fundamental natural frequency of square cross-ply laminated composite plates are presented in Table 1. Varying the length-to-thickness ratio, the results are well converged up to the elasticity (exact) solutions [13]. Considering the accuracy and computational efficiency, a 10×10 mesh in a full plate is used in examples 5.1–5.4 although further refinement of the mesh can obtain improved solutions.

Table 2 shows a comparison of the natural frequencies of laminated plates with other solutions. It is seen that the solutions obtained from the present elements are very close to exact solutions. Moreover the results of other theories are also acceptable.

5.2. Free vibration analysis of a five-ply plate (0°/0°/0°/0°/0°) with simply-free conditions at two opposite edges has been considered

This plate is simply supported along the edges parallel to the y-axis while the other two edges are free. This laminated plate has ply of thickness $0.1h/0.25h/0.15h/0.2h/0.3h$ of materials 1/2/3/1/3 [13].

Material 1: $E_1 = E_2 = E_3 = 6.9\,\text{GPa}$, $G_{12} = G_{13} = G_{23} = 1.38\,\text{GPa}$, $v_{12} = v_{13} = v_{23} = 0.25$.

Material 2: $E_1 = 224.25\,\text{GPa}$, $E_2 = E_3 = 6.9\,\text{GPa}$, $G_{12} = G_{13} = 56.58\,\text{GPa}$, $G_{23} = 1.38\,\text{GPa}$, $v_{12} = v_{13} = v_{23} = 0.25$.

Material 3: $E_1 = 172.5\,\text{GPa}$, $E_2 = E_3 = 6.9\,\text{GPa}$, $G_{12} = G_{13} = 3.45\,\text{GPa}$, $G_{23} = 1.38\,\text{GPa}$, $v_{12} = v_{13} = v_{23} = 0.25$.

The mass density $\rho = 1578\,\text{kg/m}^3$ is taken to be uniform in the thickness direction. The natural frequencies are normalized as $\Omega = \omega LS\sqrt{\rho/E_0}$, herein $E_0 = 6.9\,\text{GPa}$ and $S = L/h$.

Table 1
Convergence of the fundamental frequency

L/h	Mesh density				
	4×4	8×8	10×10	12×12	Exact [13]
5	6.85948	6.82068	6.81613	6.81367	6.8060
10	9.49984	9.38814	9.37477	9.36754	9.3434
20	10.88367	10.71066	10.68966	10.67827	10.640

Table 2
Comparison of non-dimensional frequencies of a square plate

Modes (m)	L/h	Exact [13]	Present	ZIGT [13]	TOT [13]	FSDT [13]
1	5	6.8060	6.81613	6.81281	6.97615	7.44576
	10	9.3434	9.37477	9.3434	9.47421	9.76385
	20	10.640	10.68966	10.640	10.6932	10.7890
2	5	16.515	16.61537	16.72970	16.8783	18.2491
	10	27.224	27.32669	27.25122	27.90460	29.78306
	20	37.374	37.68099	37.374	37.89724	39.05583
3	5	26.688	27.42119	27.86227	27.14169	28.76966
	10	46.419	46.66093	46.65109	47.62589	51.47867
	20	71.744	72.61932	71.744	73.25062	77.05305
4	5	37.255	39.82295	40.90599	38.18637	41.16677
	10	66.058	66.68984	66.91675	67.51127	72.99409
	20	108.89	110.53756	108.99889	111.61225	119.12566
5	5	48.035	54.19840	56.15292	50.34068	49.28391
	10	86.169	87.79897	88.409393	87.72004	94.18272
	20	147.04	149.6296	147.48112	150.86304	162.4792

Table 3
Comparison of nondimensional frequencies of a square plate with different ply thickness and material property

Modes (m)	L/h	Exact [13]	Present	ZIGT [13]	TOT [13]	FSDT [13]
1	5	7.2551	7.58558	7.28412	10.75931	10.95520
	10	10.152	10.4155	10.1723	12.17225	12.24331
	20	11.924	12.0567	11.93592	12.63944	12.65136
2	5	18.837	19.11600	19.42095	31.68383	32.90824
	10	29.020	29.91185	29.13608	43.03666	43.8202
	20	40.606	41.73284	40.68721	48.68659	48.97083
3	5	32.769	34.08000	36.17698	54.10162	56.55929
	10	50.832	52.50344	51.39115	83.16115	85.65192
	20	76.577	79.68518	76.80673	103.60868	104.83391
4	5	47.602	51.87966	58.16964	76.68682	80.01896
	10	75.349	75.65994	77.68482	126.73702	131.63470
	20	116.08	119.9550	116.54432	172.14664	175.2808
5	5	61.289	73.08509	85.37558	99.47205	103.14938
	10	102.30	105.61114	108.6426	171.4548	178.8204
	20	158.83	165.86774	159.30649	249.52193	255.7163

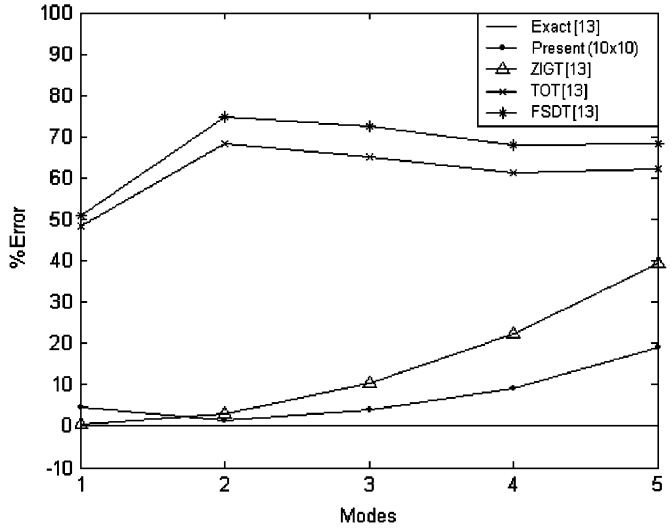

Fig. 3. Comparison of the corresponding errors for all theories ($L/h = 5$).

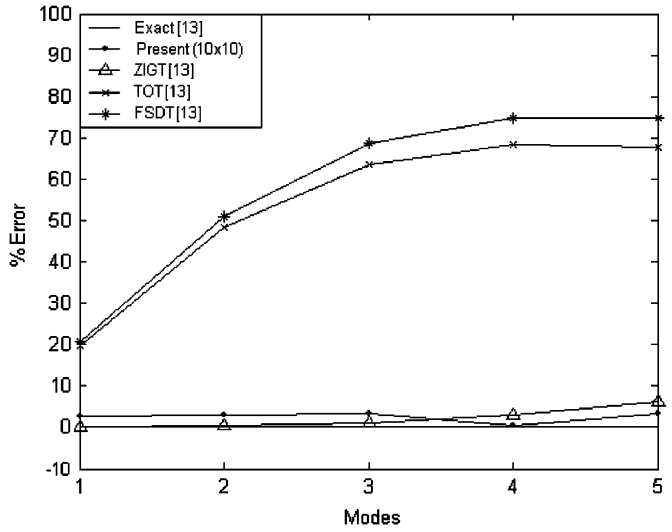

Fig. 4. Comparison of the corresponding errors for all theories ($L/h = 10$).

In the second example, a laminated composite plate with different thickness and materials at each ply is analyzed. The present normalized natural frequencies are compared with results obtained from other models in Table 3. It can be found that the present results are in good agreement with the exact solutions whereas the third-order (TOT) and first-order (FSDT) theory overestimate the frequency. However, for some higher modes, the solutions from present elements are less accurate because present theory violates the interlaminar continuity for transverse normal stress. Transverse normal stress effects on dynamical response of multilayered plates have been studied in detailed by Carrear [31]. In order to clearly compare the present theory with other theories, the corresponding errors are plotted in Figs. 3 and 4. It should be shown that for higher modes, the ZIGT in Fig. 3 are still less accurate than the present theory, which is based on the zig-zag one-dimensional theory of laminated beams.

5.3. Natural frequency of cross-ply laminated composite plate with simply supported edges is analyzed

The material properties of the individual layers are chosen as follows:

$$E_1/E_2 = \text{open},\ \ E_3 = E_2,\ \ G_{12} = G_{13} = 0.6E_2,\ G_{23} = 0.5E_2,\ v_{12} = v_{13} = v_{23} = 0.25.$$

The material properties are assumed to be the same for all layers and the fiber orientations is alternately used between 0° and 90° with respect to the x-axis. The thickness of each layer is identified and the mass density ρ is also taken to be uniform in the thickness direction. The natural frequencies are normalized as $\Omega = \omega h\sqrt{\rho/E_2}$.

In this example, both symmetric and antisymmetric laminates with respect to middle plane have been analyzed. Thereinto, the antisymmetric laminated plates have even number of layers and the 0° and layers are at the bottom and upper surfaces of the laminates, respectively. Firstly, the effects of numbers of layers and the degree of orthotropy of individual layers on dimensionless lowest frequency have been studied. These results are shown in Table 4, which are also compared with the previously published results. It is observed that the present results agree well with the 3D elasticity solutions [28]. At the same time, the fundamental frequencies of laminated plates for various values of the length-to-thickness ratio are compared with those of other models in Table 5. Numerical results show the present methods are suitable for thick laminated plates as well as thin plates.

The interlaminar stresses are the important effects on the vibration response and delamination phenomena of laminated composite plates, so the prediction of modal stresses under vibration is the important research topics in the analysis of the mechanical behavior of laminated structures [9–11,14,18]. Herein, Figs. 5–8 present the modal displacements and modal stresses. Thereinto, modal transverse shear stresses in Fig. 8 are computed directly from constitutive equation without using any postprocessing methods.

Table 4
Comparison of fundamental frequency of a simply supported plate with $L/h = 5$ ($\Omega \times 10$)

No. of layers	Solutions	E_1/E_2				
		3	10	20	30	40
2	Exact [28]	2.5031	2.7938	3.0698	3.2705	3.4250
	Present	2.5052	2.8003	3.0798	3.2838	3.4418
	Matsunaga [9]	2.4929	2.7825	3.0576	3.2578	3.4120
3	Exact [28]	2.6474	3.2841	3.8241	4.1089	4.3006
	Present	2.6344	3.2709	3.6978	3.9351	4.0928
	Matsunaga [9]	2.6276	3.2664	3.6967	3.9362	4.0951
4	Exact [28]	2.6182	3.2578	3.7622	4.0660	4.2719
	Present	2.6127	3.2513	3.7523	4.0532	4.2568
	Matsunaga [9]	2.6021	3.2380	3.7400	4.0425	4.2477
5	Exact [28]	2.6587	3.4089	3.9792	4.3140	4.5374
	Present	2.6495	3.3754	3.9133	4.2262	4.4349
	Matsunaga [9]	2.6384	3.3621	3.9012	4.2156	4.4257
6	Exact [28]	2.6440	3.3657	3.9359	4.2783	4.5091
	Present	2.6380	3.3612	3.9318	4.2747	4.5062
	Matsunaga [9]	2.6265	3.3435	3.9101	4.2505	4.4800
9	Exact [28]	2.6640	3.4432	4.0547	4.4210	4.6679
	Present	2.6559	3.4273	4.0271	4.3853	4.6271
	Matsunaga [9]	2.6452	3.4143	4.0157	4.3762	4.6198
10	Exact [28]	2.6583	3.4250	4.0337	4.4011	4.6498
	Present	2.6511	3.4183	4.0259	4.3923	4.6406
	Matsunaga [9]	2.6403	3.4044	4.0125	4.3802	4.6294

Table 5
Comparison of lowest natural frequency with previously results ($\Omega \times (\mathrm{L/h})^2$, $E_1 = 40E_2$)

Layers	Solutions	L/h							
		2	4	5	10	20	25	50	100
0/90/90/0	Present	5.4300	9.2406	10.7294	15.1658	17.8035	18.2404	18.9022	19.1566
	Wu et al. [18]	5.317	9.193	10.682	15.069	17.636	18.055	18.670	18.835
	Matsunaga [9]	5.3211	9.1988	10.6876	15.0721	17.6369	18.0557	18.6702	18.8352
	Cho et al. [16]	5.923	—	10.673	15.066	17.535	18.054	18.670	18.835

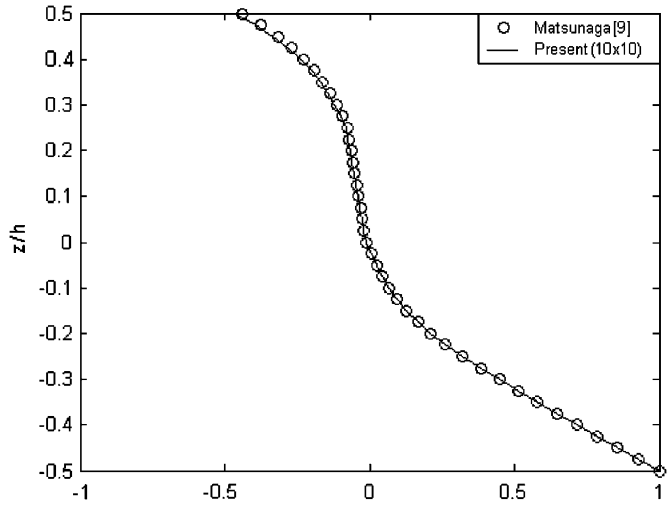

Fig. 5. Modal displacement $u/|u|_{\max}$ through thickness of four-layer plate ($L/h = 10/3$).

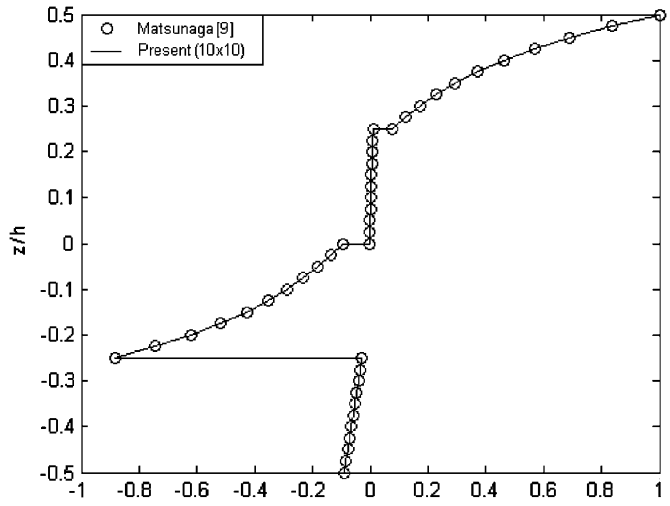

Fig. 6. Modal in-plane stress $\sigma_x/|\sigma_x|_{\max}$ through thickness of four-layer plate ($L/h = 10/3$).

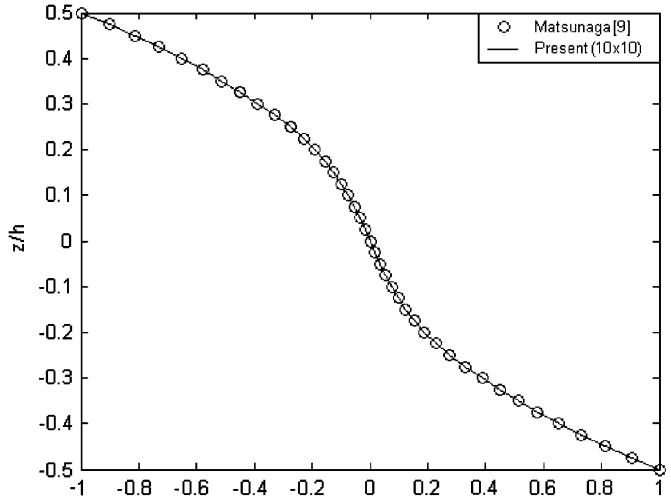

Fig. 7. Modal in-plane stress $\tau_{xy}/|\tau_{xy}|_{\max}$ through thickness of four-layer plate ($L/h = 10/3$).

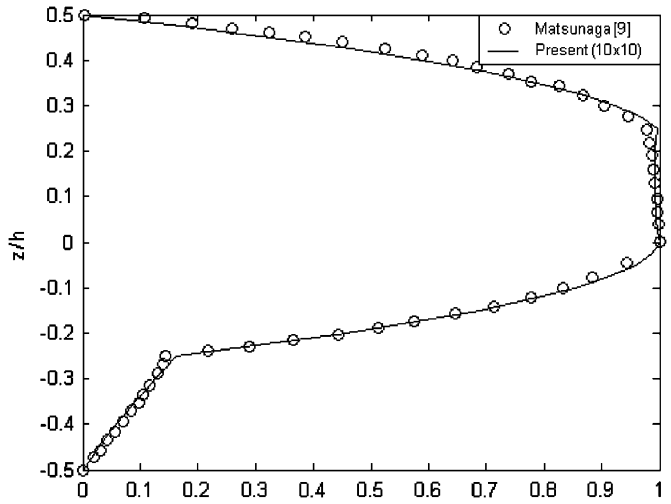

Fig. 8. Modal transverse shear stress $\tau_{xz}/|\tau_{xz}|_{\max}$ through thickness of four-layer plate ($L/h = 10/3$).

5.4. Free vibration analysis of a five-layer (0°/90°/core/0°/90°) sandwich plate has been presented in this example

The ratio of thickness of core t_c to thickness of face sheet t_f has been used to be 10. The following material properties are adopted [14]:

Face sheets: $E_1 = 131\,\text{GPa}$, $E_2 = E_3 = 10.34\,\text{GPa}$, $G_{12} = G_{23} = 6.895\,\text{GPa}$,

$$G_{13} = 6.205\ \text{GPa},\ \ v_{12} = v_{13} = 0.22,\ \ v_{23} = 0.49,\ \ \rho = 1627\ \text{kg/m}^3,$$

Core (isotropic): $E_1 = E_2 = E_3 = 6.89 \times 10^{-3}\,\text{GPa}$, $G_{12} = G_{13} = G_{23} = 3.45 \times 10^{-3}\,\text{GPa}$ $v_{12} = v_{13} = v_{23} = 0$, $\rho = 97\,\text{kg/m}^3$.

The natural frequencies are normalized as $\Omega = \omega L^2(\rho/E_2)_f^{1/2}/h$.

To further assess the range of applicability of the present global–local theory, a problem on soft-core sandwich plates has been considered. Due to large difference in stiffness between the face sheets and the core material, the analysis on sandwich plates needs a refined laminated plate theory.

The present solutions for moderately thick plate and thin plate are given in Table 6, which are also compared with semi-analytical results obtained from mixed theories [14] and displacement-based analytical

Table 6
Comparison of non-dimensional frequencies of sandwich plate

L/h	Modes	Rao(LW) [14]	Present	Rao(ESL) [14]	Kant et al. [6]	Pandya, Kant [6]	Reddy [6]	Senthilnathan et al. [6]	Whitney Panano [6]
10	1,1	1.8480	1.94445	4.9624	4.8594	4.8519	7.0473	7.0473	13.8694
	1,2	3.2196	3.37955	8.1934	8.0187	7.9965	11.9087	11.9624	30.6432
	2,2	4.2894	4.59140	11.9867	10.2966	10.2550	15.2897	15.2897	41.5577
	1,3	5.2236	5.52678	10.5172	11.7381	11.6809	17.3211	17.3698	50.9389
	2,3	6.0942	6.51279	13.7488	13.4706	13.3889	19.8121	19.8325	58.3636
	3,3	7.6762	8.43110	16.4514	16.1320	16.0039	23.5067	23.5067	71.3722
100	1,1	11.9401	11.9840	15.5480	15.5093	15.4646	15.9521	15.9521	16.2175
	1,2	23.4017	23.3427	39.2652	39.0293	38.9232	42.2271	42.3708	44.7072
	2,2	30.9432	31.8651	55.1512	54.7618	54.6330	60.1272	60.1272	64.5044
	1,3	36.1434	36.5671	73.4951	72.7572	72.5925	83.9982	84.4251	94.9097
	2,3	41.4475	42.2904	84.2919	83.4412	83.2699	96.3132	96.7159	108.9049
	3,3	49.7622	50.0815	106.5897	105.3781	105.1807	124.2047	124.2047	143.7969

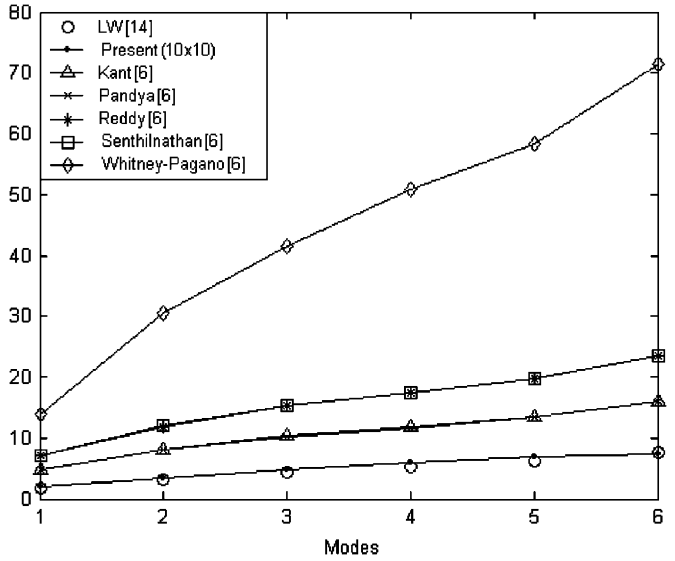

Fig. 9. Comparison of the corresponding frequencies for all theories ($L/h = 10$).

results [6]. It can be found from Table 6 that the present results agree well with those obtained by mixed layerwise model for thick ($L/h = 10$) as well as thin ($L/h = 100$) sandwich plate whereas other global higher- and first-order theories overestimate the natural frequencies. The advantage of the global–local higher-order theory can be found clearly by numerical comparison. At the same time, Figs. 9 and 10 show the clear comparison of all results.

5.5. *Free vibration analysis of the three-layer clamped plate ($0^\circ/90^\circ/0^\circ$) has been considered*

The following material properties are adopted [29,30]:

$$E_1/E_2 = 40,\ \ E_3 = E_2,\ G_{12} = G_{13} = 0.6E_2,\ G_{23} = 0.5E_2,$$

$$v_{12} = v_{13} = v_{23} = 0.25,\ v_{21} = 0.00625.$$

In this case, a and b are the length and width of laminated plate, respectively; h is the thickness of laminates. The natural frequencies are normalized as $\Omega = (\omega b^2/\pi^2)\sqrt{(\rho h/D_0)}$, where $D_0 = E_2h^3/12(1 - v_{12}v_{21})$.

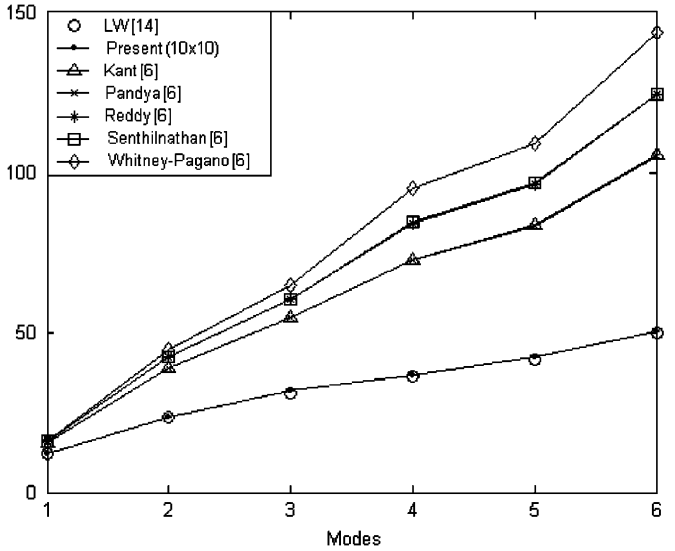

Fig. 10. Comparison of the corresponding frequencies for all theories ($L/h = 100$).

Table 7
Comparison of natural frequency for a three-layer clamped plate (0°/90°/0°)

a/b	b/h	Mode sequence number							
			1	2	3	4	5	6	7	8
1	5	Liew [29]	4.447	6.642	7.700	9.185	9.738	11.399	11.644	12.466
		Present	4.540	6.524	8.178	9.473	9.492	11.769	12.395	12.904
	10	Liew [29]	7.411	10.393	13.913	15.429	15.806	19.572	21.489	21.620
		Jian et al. [30]	7.451	10.451	13.993	15.534	15.896	19.698	21.618	21.773
		Present	7.484	10.207	14.340	14.863	16.070	19.508	20.716	22.489
	20	Liew [29]	10.953	14.028	20.388	23.196	24.978	29.237	29.369	36.266
		Jian et al. [30]	11.015	14.152	20.691	23.323	25.142	29.532	29.777	36.665
		Present	11.003	14.064	20.321	23.498	25.350	29.118	29.679	36.624
	100	Liew [29]	14.666	17.614	24.511	35.532	39.157	40.768	44.786	50.297
		Jian et al. [30]	14.583	17.762	25.004	36.644	38.073	39.802	44.082	51.725
		Present	14.601	17.812	25.236	37.168	38.528	40.668	45.724	53.271
2	5	Liew [29]	3.045	4.248	5.792	5.905	6.535	7.688	7.729	9.176
		Present	2.953	4.288	5.595	6.096	6.446	7.796	8.053	9.005
	10	Liew [29]	4.141	6.617	8.354	9.895	9.967	12.443	13.659	14.120
		Jian et al. [30]	4.164	6.652	8.401	9.950	10.023	12.513	13.743	14.221
		Present	4.119	6.705	8.240	9.916	10.212	12.671	14.066	14.082
	20	Liew [29]	4.779	8.840	9.847	12.511	14.703	17.300	17.673	19.429
		Jian et al. [30]	4.838	8.910	9.982	12.647	14.824	17.467	17.996	19.744
		Present	4.813	8.954	9.968	12.768	14.960	17.764	18.041	19.993
	100	Liew [29]	5.105	10.527	10.583	14.324	19.567	19.701	22.148	22.237
		Jian et al. [30]	5.250	10.697	11.012	14.726	19.697	20.420	22.445	22.933
		Present	5.144	10.407	10.929	14.706	18.954	20.799	22.205	23.703

In this case, a 12×12 mesh in a full plate is used and the solutions are presented for the rectangular clamped plates with various thickness and aspect ratios, namely b/h and a/b. It is seen that the present solutions of the global–local higher-order theory agree well with those of other theories [29,30] in Table 7.

6. Conclusions

Natural frequencies of laminated composite and sandwich plates have been calculated by using the global–local higher-order theory, and these results are compared with those previously published. These comparisons revealed that the present theory can accurately predict natural frequencies of general laminated plates. Moreover, this theory is still suitable for dynamical problems of laminated composite plates with variational thickness and materials at each layer and soft-core sandwich plates. However, numerical results show that for these special structures, the global higher- and first-order theories that violate continuity of interlaminar stresses will encounter some difficulties and overestimate the natural frequencies.

On the other hand, the distribution of modal displacements and stresses in thickness direction has been also presented in the ply level. Thereinto the modal transverse shear stresses have been calculated directly from the constitutive equations without any postprocessing methods.

References

[1] A.K. Noor, W. Scott Burton, Stress and free vibration analysis of multilayered composite plates, *Composite Structures* 11 (1989) 183–204.
[2] C.M. Wang, Vibration frequencies of simply-supported polygonal sandwich plates via Kirchhoff solution, *Journal of Sound Vibration* 2 (1996) 255–260.
[3] J.N. Reddy, A simple higher-order theory for laminated composite plates, *Journal of Applied. Mechanics* 51 (1984) 745–752.
[4] P.S. Frederiksen, Single-layer plate theories applied to the flexural vibration of completely free thick laminates, *Journal of Sound and Vibration* 186 (5) (1995) 743–759.
[5] D.K. Maiti, P.K. Sinha, Bending, free vibration and impact response of thick laminated composite plates, *Computers & Structures* 59 (1) (1996) 115–129.
[6] T. Kant, K. Swaminathan, Free vibration of isotropic, orthotropic, and multilayer plates based on higher order refined theories, *Journal of Sound and Vibration* 241 (2) (2001) 319–327.
[7] T. Kant, K. Swaminathan, Analytical solutions for free vibration of laminated composite and sandwich plates based on a higher-order refined theory, *Composite Structrues* 53 (2001) 73–85.
[8] S.-Y. Lee, S.-C. Wooh, S.-S. Yhim, Dynamic behavior of folded composite plates analyzed by the third order plate theory, *International Journal of Solids and Structrues* 41 (2004) 1879–1892.
[9] H. Matsunaga, Vibration and stability of cross-ply laminated composite plates according to a global higher-order plate theory, *Composite Structures* 48 (2000) 231–244.
[10] H. Matsunaga, Vibration and stability of angle-ply laminated composite plates subjected to in-plane stresses, *International Journal of Mechanical Sciences* 43 (2001) 1925–1944.
[11] H. Matsunaga, Vibration of cross-ply laminated composite plates subjected to initial in-plane stresses, *Thin-Walled Structures* 40 (2002) 557–571.
[12] A.K. Nayak, S.S.J. Moy, R.A. Shenoi, Free vibration analysis of composite sandwich plates based on Reddy's higher-order theory, *Composites: Part B* 33 (2002) 505–519.
[13] S. Kapuria, P.C. Dumir, N.K. Jain, Assessment of zig-zag theory for static loading, buckling, free and forced response of composite and sandwich beams, *Composite Structures* 64 (2004) 317–327.
[14] M.K. Rao, Y.M. Desai, Analytical solutions for vibrations of laminated and sandwich plates using mixed theory, *Composite Structures* 63 (2004) 361–373.
[15] R.R. Valisetty, L.W. Rehfield, Application of ply level analysis to flexure wave vibration, *Journal of Sound and Vibration* 126 (1988) 183–194.
[16] K.N. Cho, C.W. Bert, A.G. Striz, Free vibration of laminated rectangular plates analyzed by higher-order individual-layer theory, *Journal of Sound and Vibration* 145 (1991) 429–442.
[17] A. Noiser, R.K. Kapania, J.N. Reddy, Free vibration analysis of laminated plates using a layer-wise theory, *AIAA Journal* 31 (1993) 2335–2346.
[18] C.P. Wu, W.Y. Chen, Vibration and stability of laminated plates based on a local higher-order plate theory, *Journal of Sound and Vibration* 177 (4) (1994) 503–520.
[19] E. Carrera, Layerwise mixed models for accurate vibrations analysis of multilayered plates, *Journal of Applied Mechanics* 65 (1998) 820–828.
[20] M.K. Rao, Y.M. Desai, M.R. Chitnis, Free vibrations of laminated beams using mixed theory, *Composite Structures* 52 (2001) 149–160.
[21] X.Y. Li, D. Liu, Generalized laminate theories based on double superposition hypothesis, *International Journal of Numerical Methods Engineering* 40 (1997) 1197–1212.
[22] W. Zhen, C. Ronggeng, C. Wanji, Refined laminated composite plate element based on global-local higher-order shear deformation theory, *Composite Structrues* 70 (2005) 135–152.

[23] W. Zhen, C. Wanji, An efficient higher-order theory and finite element for laminated plates subjected to thermal loading, *Composite Structures* 73 (2006) 99–109.
[24] C. Wanji, Nine-parameter triangular thin plate bending element by using refined directed stiffness method, *Journal of Dalian University of Technology* 33 (2) (1993) 289–295 (in Chinese).
[25] Y.K. Cheung, Chen Wanji, Refined nine-parameter triangular thin plate bending element by using refined direct stiffness method, *International Journal for Numerical Methods in Engineering* 38 (1995) 283–298.
[26] G.P. Bazeley, Y.K. Cheung, B.M. Irons, O.C. Zienkiewiz, Triangular elements in bending conforming and non-conforming solution, *Proceedings of the Conference on Matrix Methods in Structural Mechanics, Air Force Ins. Tech., Wright-Patterson A.F. Base, OH* (1965) 547–576.
[27] K.J. Bathe, *The Finite Element Procedures in Engineering Analysis*, Prentice-Hall, Prentice, NJ, 1996.
[28] A.K. Noor, Mixed finite-difference scheme for analysis of simply supported thick plates, *Computers & Structures* 3 (1973) 967–982.
[29] K.M. Liew, Solving the vibration of thick symmetric laminates by Reissner/Mindlin plate theory and the p-Titz method, *Journal of Sound and Vibration* 198 (1996) 343–360.
[30] W.S. Jian, A. Nakatani, H. Kitagawa, Vibration analysis of fully clamped arbitrarily laminated plate, *Composite Structures* 63 (2004) 115–122.
[31] E. Carrera, A study of transverse normal stress effects on vibration of multilayered plates and shells, *Journal of Sound and Vibration* 225 (1999) 803–829.